

ISSN: 0256-307X

# 中国物理快报

# Chinese Physics Letters

Volume 28 Number 8 August 2011

A Series Journal of the Chinese Physical Society  
Distributed by IOP Publishing

Online: <http://iopscience.iop.org/cpl>  
<http://cpl.iphy.ac.cn>

**CHINESE PHYSICAL SOCIETY**  
Institute of **Physics** PUBLISHING

JUST FOR AUTHORS  
— CHINESE PHYSICS LETTERS

## Elimination of the Coherent Artifact in a Pump-Probe Experiment by Directly Detecting the Background-Free Diffraction Signal \*

LIU Hui(刘晖), ZHANG Hang(张航), SI Jin-Hai(司金海)\*\*, YAN Li-He(闫理贺), CHEN Feng(陈烽),  
HOU Xun(侯洵)

Key Laboratory for Physical Electronics and Devices of the Ministry of Education & Shaanxi Key Lab of Information Photonic Technique, School of Electronics & information Engineering, Xi'an Jiaotong University, Xi'an 710049

(Received 17 May 2011)

*The influence of the coherent artifact in a semiconductor Ga-doped ZnO film on femtosecond pump-probe measurement is studied. The coherent artifact mixed into the pump-probe signal can be directly inspected by detecting the background-free first-order diffraction signal induced by the interference between the pump and probe pulses. Experimental results show that by varying the polarization angle or adjusting the relative intensity between the pump and probe pulses, the coherent artifact can be eliminated from the pump-probe measurement.*

PACS: 66.30.Fq, 82.53.Eb, 42.65.Re

DOI:10.1088/0256-307X/28/8/086602

The degenerate pump-probe technique has been applied to time-resolved measurements over the past decades.<sup>[1–9]</sup> Observing ground-state bleaching and excited-state absorption or stimulated emission through transient absorption experiments is widely applied in investigations of the carrier dynamic process of organic materials, semiconductors and other materials.<sup>[10,11]</sup> During the degenerate pump-probe process, however, the coherent artifact can be easily formed around zero delay time between the pump and probe pulses.<sup>[12,13]</sup> This phenomenon is explained by the diffraction from a transient grating induced by interference between the pump and probe beams.<sup>[14–17]</sup> When the pump and probe pulses are temporally overlapped, the interference between the pump and probe pulses leads to a transient refractive-index grating due to the nonlinear effect in non-resonance materials.<sup>[18–20]</sup> In a resonance material, the interference pattern of two coherent pulses can generate a periodic spatial distribution of the carrier concentration.<sup>[21–23]</sup> This spatial periodicity of the free electrons and holes causes a similar periodic perturbation in the refractive index.<sup>[24]</sup>

The two kinds of grating described above lead to a diffraction of the pump beam into the probe beam.<sup>[25,26]</sup> Indeed, this coherent artifact can be found in most time-resolved degenerate pump-probe experiments. Experimentally, the diffraction signal of the pump beam mixed into the probe beam is overlapped with the pump-probe trace, which disturbs the analysis of relaxation dynamics to determine the amplitude of the signal and relaxation.<sup>[18,27–30]</sup>

In this Letter, the influence of the coherent arti-

fact on femtosecond pump-probe measurement is studied in semiconductor Ga-doped ZnO film. The coherent artifact mixed into the pump-probe signal can be directly inspected by detecting the background-free first-order diffraction signal induced by the interference between the pump and probe pulses. Experimental results show that by varying the polarization angle or adjusting the relative intensity between the pump and probe pulses, the coherent artifact can be eliminated from the pump-probe measurement.

The ZnO:Ga film was fabricated by radiofrequency (rf, 13.56 MHz) magnetron sputtering technique. The target for the rf magnetron sputtering process is prepared by cold pressing and subsequent sintering of a mixture of ZnO and Ga<sub>2</sub>O<sub>3</sub> powders (both 5N) with a 95:5 molar ratio of Zn:Ga in a oxygen atmosphere at 1050°C for 12 h. The process chamber was a custom-built rf magnetron sputtering chamber with a base pressure of  $6.67 \times 10^{-5}$  Pa. A ZnO:Ga target was used for sputtering with a flux ratio of Ar:O<sub>2</sub>=3:1, the rf power was 150 W. The distance between the substrate and target was 12 cm. The deposition rate was about 22 nm/min (the rf power was 150 W). The double smoothed sapphire substrate was degreased both in acetone and in methanol, each for 10 min at room temperature, then etched in HF for 1–2 s, followed by rinsing in deionized water and drying with a 5N nitrogen. After a thermal cleaning of the sapphire substrate at 600°C, a 100-nm-thick ZnO:Ga buffer layer was deposited at the rf power of 100 W on a double smoothed and cleaned sapphire substrate. The buffer layer sputtering was carried out at room temperature. The chamber deposition pressure was 1 Pa. Then a

\*Supported by the National Natural Science Foundation of China under Grant No 11074197, and the Specialized Research Fund for the Doctoral Program of Higher Education of China under the Grant No 200806980022.

\*\*Correspondence author. Email: jinhaishi@mail.xjtu.edu.cn

© 2011 Chinese Physical Society and IOP Publishing Ltd

2- $\mu\text{m}$ -thick ZnO:Ga film was deposited on the buffer layer using the rf magnetron sputtering technique at a substrate temperature 350°C. The ZnO:Ga film was annealed at 600°C under a 1 Pa nitrogen pressure for 40 min and then cooled down under it.

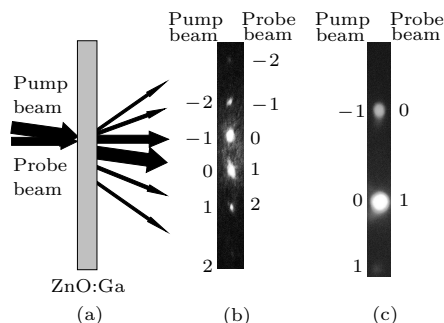


**Fig. 1.** (a) The diffraction geometry. (b) CCD image of the diffraction pattern of transmitted light with pump power at 7 mW and probe power at 7 mW. (c) CCD image of the diffraction pattern of transmitted light with pump power at 7 mW and probe power at 1 mW. The minus first-order pump and zero-order probe fall together, and so on, as indicated. The first-order pump and zero-order probe are detected by PMT.

The multi-pass amplified Ti:sapphire laser emitting 30 fs, 800 nm laser pulses at a repetition rate of 1 kHz was split into two beams. One was served as the probe beam and focused into a ZnO:Ga film with thickness 2  $\mu\text{m}$  by a 10-cm focal-length lens. The other (pump beam) passed through a time-delay device and a  $\lambda/2$  plate to control the path length and polarization of the pump beam, respectively. Both beams were focused by lenses before passing through the ZnO:Ga film. The centers of the pump and the probe beams spatially overlapped at the ZnO:Ga film at an angle of 12°. The probe beam was focused into the photomultiplier tube (PMT) while the first diffracted order of the pump beam was collected into another PMT. An infrared filter was used to remove the luminescence at about 395 nm on the ZnO:Ga film mixed in the detected beam. As the time-delay device moves, the two temporal signals can be simultaneously detected.

The pump and probe pulses form the transient grating induced by two-photon absorption of two interfering optical beams in the ZnO:Ga film.<sup>[31]</sup> The pump and probe beams were simultaneously diffracted by this transient grating. The diffraction geometry is shown in Fig. 1(a). Figure 1(b) shows the diffraction patterns imaged by a CCD with the power of both pump and probe beams fixed at 7 mW. From Fig. 1(b), the multi-order diffraction patterns can be clearly observed. The multi-order diffraction patterns are distributed symmetrically on both sides of the pump and probe beams in space. The minus first-order diffraction of the pump beam, which is mixed into the probe beam, is located in the mirror direction of the first

order diffraction. The detection on the first-order diffraction of the pump beam, which is different from the transmitted direction of the probe beam, may be more direct and convenient to present the existence of the coherent artifact. When the probe power decreases down to 1 mW, only the first-order diffraction of the pump beam can be seen, as shown in Fig. 1(c). The minus first-order diffraction of the pump beam is always mixed into the probe beam.

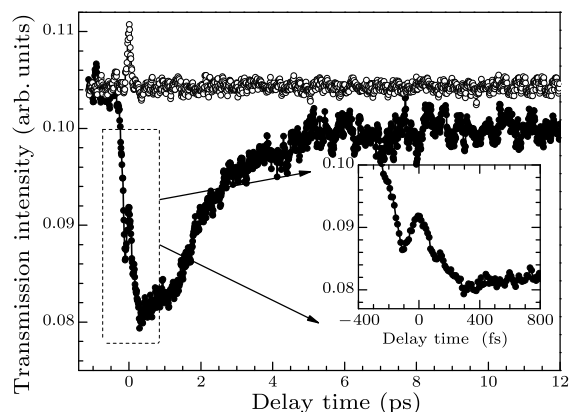


**Fig. 2.** Time-resolved profile of the first-order diffraction of the pump beam (open circles) and the probe transmission (closed circles). The pump power and probe power are set at 7 mW and 1 mW, respectively. The inset shows the enlarged map of the trace in the dashed rectangle.

To temporally investigate the relationship between the coherent artifact and the first-order diffraction of the pump beam, the time-resolved temporal profile of the first-order diffraction of the pump beam and the probe transmission were measured, in which the pump power and probe power were set at 7 mW and 1 mW, respectively. The results are shown in Fig. 2. We can see the dramatic variation of the transmission around zero delay time, which can be attributed to the strong coherent artifact. The inset shows the enlarged map of the trace in the dashed rectangle. The full width at half maximum (FWHM) of the coherent artifact signal is 110 fs, which is the same as that of the incident pulse autocorrelation. Namely, the coherent artifact can be observed only in the temporal overlapping region of pump and probe pulses. The rising part of the pump-probe trace consists of three processes. The process within the first 1 ps corresponds to the free carrier absorption, which implies the cooling of the hot carriers to a quasi-thermal equilibrium with time constant 1 ps. The slow decay process with the time constant more than 9 ps appears after 3 ps, which is attributed to spontaneous emission. The process from 1 to 3 ps represents the electron-hole plasma (EHP) radiation recombination, in which the carrier concentration should be higher than the Mott transition density of about  $10^{18} \text{ cm}^{-3}$ .<sup>[32]</sup> When the car-

rier concentration decreases below the Mott transition density, the slow decay process related to the spontaneous emission will be dominant.

The result indicated by open circles in Fig. 2 shows the time-resolved profile of the first-order diffraction of the pump beam. The first-order diffraction of the pump beam temporally presents near the zero time delay, the FWHM is also 110 fs. The first-order diffraction of the pump beam disappears while the pump and probe pulses are slightly separated temporally.

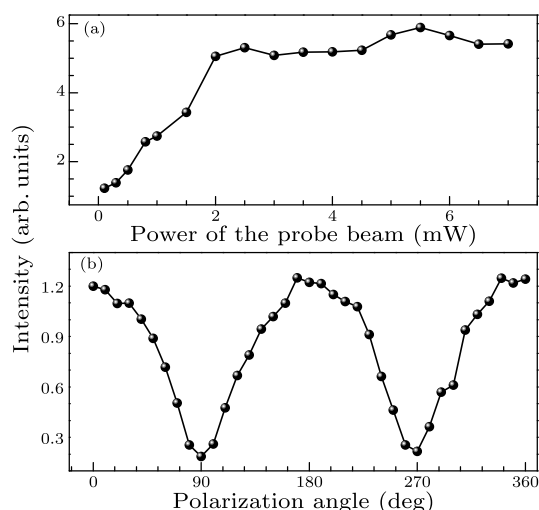


**Fig. 3.** (a) Dependence of the intensity of the first-order diffraction of the pump beam on the power of the probe beam. The pump power is set at 7 mW. (b) Dependence of the intensity of the first-order diffraction of the pump beam on the polarization angle between the pump beam and the probe beam.

The coherent artifact appears simultaneously with the first-order diffraction of the pump beam at zero time delay. In a degenerate pump-probe configuration, the first-order diffraction of the pump beam is the mirror component of the minus first-order diffraction of the pump beam. They both have the same frequency but different directions. The influence of the coherent artifact can be discriminated by directly inspecting the background-free first-order diffraction of the pump beam.

Since the transient grating is induced by two-photon absorption of two interfering optical beams, the interference of the pump and probe pulses can be weakened drastically by decreasing the probe power. Figure 3(a) shows the dependence of the intensity of the first-order diffraction of the pump beam on the power of the probe beam, in which the polarization angle between the pump and probe beams is set at  $0^\circ$ . It indicates that the diffraction intensity increases with increasing probe power when the probe power is below 2 mW. The diffraction intensity approaches its saturation value when the probe power is increased to 2 mW. The experimental results described above

indicate that the coherent artifact in the pump-probe measurements can be suppressed by a reduction of the power of the probe beam.

Further, we also measured the dependence of intensity of the first-order diffraction of the pump beam on the polarization angle between the pump and probe beams, and the results are shown in Fig. 3(b). We can see that the dependence of the diffraction intensity on the polarization angle displays a periodic change. The change period of the diffraction intensity is  $\pi$ . The diffraction intensity presents strongest as the polarization angle of the pump and probe beams is set at  $0^\circ$  or  $180^\circ$ , and the diffraction intensity becomes weakest as the polarization angle of the pump and probe beams is set at  $90^\circ$  or  $270^\circ$ . The diffraction intensity can be eliminated by setting the polarization angle of the pump and probe beams to be orthogonal.

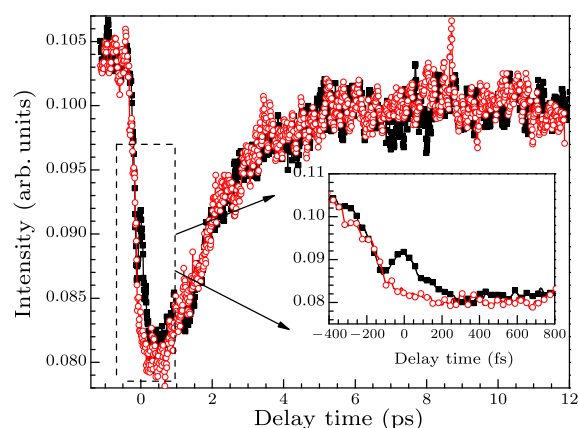


**Fig. 4.** Time-resolved profile of probe transmission with different probe powers. The pump power is set at 7 mW, and the probe power is set at 1 mW (closed circles) and 0.2 mW (open circles). The inset shows an enlarged region of the data in the dashed rectangle.

Figure 4 shows the time-resolved profile of the probe transmission. The polarization angle between the pump and probe beams is set at  $0^\circ$  and the pump power is set at 7 mW. The probe power is set at 1 mW and 0.2 mW, respectively. From the inset in Fig. 4, we can see that the coherent artifact for the probe power of 0.2 mW is eliminated. Generally, the coherent artifact can be eliminated by setting the orthogonal polarization between the pump beam and probe beam according to the above description. However, orthogonal polarization configuration can not be used in pump-probe measurements such as the optical Kerr shutter.<sup>[18]</sup> Therefore, for optical Kerr shutter probe-pump experiments, the coherent artifact can be eliminated by reducing the probe-to-pump power ratio.

In summary, the influence of the coherent artifact on femtosecond pump-probe measurement has been studied in semiconductor Ga-doped ZnO film. The coherent artifact mixed into the pump-probe signal can

be directly inspected by detecting the background-free first-order diffraction signal induced by the interference between the pump and probe pulses. Experimental results show that by varying the polarization angle or adjusting the relative intensity between the pump and probe pulses, the coherent artifact can be eliminated from the pump-probe measurement.

## References

- [1] Wundke K, Pötting S, Auxier J, Schülzgen A, Peyghambarian N and Borrelli N F 2000 *Appl. Phys. Lett.* **76** 10
- [2] Liu X, Liu W, Yin J, Qu J, Lin Z and Niu H 2011 *Chin. Phys. Lett.* **28** 034202
- [3] Li F, Meng F, Feng W, Wang Sh, Tian H and Gong Q 2010 *Chin. Phys. Lett.* **27** 068202
- [4] Elim H I, Ji W, Ma G H, Lim K Y, Sow C H and Huan C H A 2004 *Appl. Phys. Lett.* **85** 1799
- [5] Tsai T -R, Chang C -F and Gwo S 2007 *Appl. Phys. Lett.* **90** 252111
- [6] Gopinath J T, Thoen E R, Koontz E M, Grein M E, Kolodziejski L A, Ippen E P and Donnelly J P 2001 *Appl. Phys. Lett.* **78** 3409
- [7] Sanchez S, De Matos C and Pugnet M 2001 *Appl. Phys. Lett.* **78** 3779
- [8] Ye H, Wicks G W and Fauchet P M 2000 *Appl. Phys. Lett.* **77** 1185
- [9] Sun C -K, Vallée F, Keller S, Bowers J E and DenBaars S P 1997 *Appl. Phys. Lett.* **70** 2004
- [10] Lioudakis E, Othonos A, Dimakis E, Iliopoulos E and Georgakilas A 2006 *Appl. Phys. Lett.* **88** 121128
- [11] Si J and Hirao K 2007 *Appl. Phys. Lett.* **91** 091105
- [12] Luo C W, Wang Y T, Chen F W, Shih H C and Kobayashi T 2009 *Opt. Express* **17** 11321
- [13] Borri P, Romstad F, Langbein W, Kelly A E, Mørk J and Hvam J M 2000 *Opt. Express* **7** 107
- [14] Vandeny Z and Tauc J 1981 *Opt. Commun.* **39** 396
- [15] Palfrey S L and Heinz T F 1985 *J. Opt. Soc. Am. B* **2** 674
- [16] Sanchez F 1992 *J. Opt. Soc. Am. B* **9** 2196
- [17] Cundiff S T 2008 *Opt. Express* **16** 4639
- [18] Yan L H, Yue J J, Si J H and Hou X 2008 *Opt. Express* **16** 12069
- [19] Dogariu A, Xia T, Hagan D J, Said A A, Van Stryland E W and Bloembergen N 1997 *J. Opt. Soc. Am. B* **14** 796
- [20] Qu S, Zhao Ch, Zhao Q, Qiu J, Zhu C and Hirao K 2004 *Opt. Lett.* **29** 2058
- [21] Ravn J N 1992 *IEEE J. Quantum Electron.* **28** 315
- [22] Kalt H, Lyssenko V G, Renner R and Klingshirm C 1985 *J. Opt. Soc. Am. B* **2** 1188
- [23] Divakara Rao K and Sharma K K 1995 *J. Opt. Soc. Am. B* **12** 658
- [24] Si J, Qiu J, Zhai J, Shen Y and Hirao K 2002 *Appl. Phys. Lett.* **80** 359
- [25] Schneider Th, Wolfram D, Mitzner R and Reif J 1999 *Appl. Phys. B* **68** 749
- [26] Dean D R and Collins R J 1973 *J. Appl. Phys.* **44** 5455
- [27] Wang C -R, Luo T and Lu Q -B 2008 *Phys. Chem. Chem. Phys.* **10** 4463
- [28] Chudoba C, Nibbering E T J and Elsaesser T 1998 *Phys. Rev. Lett.* **81** 3010
- [29] Conrad U, Gdde J, Jhnke V and Matthias E 1999 *Appl. Phys. B* **68** 511
- [30] Lebedev M V, Misochko O V, Dekorsy T and Georgiev N 2005 *J. Exp. Theor. Phys.* **100** 272
- [31] Liu H, Zhang H, Si J, Zhang J, Yan L, Wei X, Wen X and Hou X 2010 *Opt. Commun.* **283** 5203
- [32] Takeda J, Jinnouchi H, Kurita S, Chen Y F and Yao T 2002 *Phys. Status Solidi B* **229** 877

JUST FOR AUTHORS  
 — CHINESE PHYSICS LETTERS

# Chinese Physics Letters

Volume 28

Number 8

August 2011

## GENERAL

- 080201 Solving Method for the Single-Kink Soliton Solution to a Disturbed Coupled Burgers System  
YAO Jing-Su, CHEN Li-Hua, WEN Zhao-Hui, MO Jia-Qi
- 080301 Geometric Phase for a Qutrit-Qubit Mixed-Spin System  
ZHANG Ai-Ping, QIANG Wen-Chao, LING Ya-Wen, XIN Hong, YANG Yong-Ming
- 080302 Implementation of Quantum Private Queries Using Nuclear Magnetic Resonance  
WANG Chuan, HAO Liang, ZHAO Lian-Jie
- 080303  $N$ -Qubit  $W$  State of Spatially Separated Atoms via Fractional Adiabatic Passage  
ZHENG An-Shou, LIU Ji-Bing, CHEN Hong-Yun
- 080401 Feasibility for Testing the Equivalence Principle with Optical Readout in Space  
GAO Fen, ZHOU Ze-Bing, LUO Jun
- 080501 Pseudo-Random Sequences Generated by a Class of One-Dimensional Smooth Map  
WANG Xing-Yuan, QIN Xue, XIE Yi-Xin
- 080502 Size Model of Critical Temperature for Grain Growth in Nano V and Au  
LU Yun-Bin, LIAO Shu-Zhi, PENG Hao-Jun, ZHANG Chun, ZHOU Hui-Ying, XIE Hao-Wen, OUYANG Yi-Fang, ZHANG Bang-Wei
- 080601 Feasibility of Extreme Ultraviolet Active Optical Clock  
ZHUANG Wei, CHEN Jing-Biao
- 080701 Micropore Structure Representation of Sandstone in Petroleum Reservoirs Using an Atomic Force Microscope  
BAI Yong-Qiang, ZHU Xing, WU Jun-Zheng, BAI Wen-Guang
- 080702 Room-Temperature  $\text{NH}_3$  Gas Sensor Based on Hydrothermally Grown ZnO Nanorods  
WEI Ang, WANG Zhao, PAN Liu-Hua, LI Wei-Wei, XIONG Li, DONG Xiao-Chen, HUANG Wei

## THE PHYSICS OF ELEMENTARY PARTICLES AND FIELDS

- 081201 Analysis of Mass Difference of the  $\pi$  and  $\rho$  with Bethe-Salpeter Equation  
WANG Zhi-Gang
- 081202 Lattice QCD Study of the  $\sigma$  Meson  
FU Zi-Wen
- 081301 Large Dimuon Asymmetry and a Non-Universal  $Z'$  Boson in the  $B_s - \bar{B}_s$  System  
CHANG Qin, WANG Ru-Min, XU Yuan-Guo, CUI Xiao-Wei
- 081401 Effect of Excited and Fourth Generation Leptons in Lepton Flavor Violating  $\mu^- \rightarrow e^- 2\gamma$  Decay  
S. C. İnan

## NUCLEAR PHYSICS

- 082501 Singly and Doubly Charged Projectile Fragments in Nucleus-Emulsion Collisions at Dubna Energy in the Framework of the Multi-Source Model  
WANG Er-Qin, LIU Fu-Hu, Magda A. Rahim, S. Fakhraddin, SUN Jian-Xin
- 082502 Comparison of Fission Induced by Protons and Pions  
Zafar Yasin, M. Ikram Shahzad
- 082801 Measurement of Cross Sections for the  $^{10}\text{B}(n, \alpha)^7\text{Li}$  Reaction at 4.0 and 5.0 MeV Using an Asymmetrical Twin Gridded Ionization Chamber  
ZHANG Guo-Hui, LIU Xiang, LIU Jia-Ming, XUE Zhi-Hua, WU Hao, CHEN Jin-Xiang
- 082901 Effects of Electron Flow Current Density on Flow Impedance of Magnetically Insulated Transmission Lines  
HE Yong, ZOU Wen-Kang, SONG Sheng-Yi

## ATOMIC AND MOLECULAR PHYSICS

- 083101 Quasi-Classical Trajectory Calculations of Reaction Stereodynamics of  $\text{H}+\text{OH}(v=0, j=0)\rightarrow\text{H}_2+\text{O}(^3P)$**   
ZHAO Li, SUN Ping, LIU Chao-Zhuo
- 083102 Product Rotational Polarization in the  $\text{Li} + \text{HF}(v=0, j=0)$  Reaction and Its Isotopic Variants**  
CHENG Jie, YUE Xian-Fang
- 083201 Intensity and Polarization Effects in Short-Pulse Multiphoton Ionization of Xenon**  
KANG Hui-Peng, WANG Chuan-Liang, LIN Zhi-Yang, CHEN Yong-Ju, WU Ming-Yan, QUAN Wei, LIU Hong-Ping, LIU Xiao-Jun
- 083202 Relative Phase Dependence of Double Ionization in a Synthesized Laser Pulse**  
WANG Yuan-Sheng, XIA Chang-Long, GUO Jing, LIU Xue-Shen
- 083203 Radiation-Induced Nano-Explosions at the Solid Surface: Near Surface Radiation Damage in CR-39 Polymer**  
Mukhtar Ahmed Rana
- 083301 Investigation of Linear Tetra-Atomic Negative Ion by Photodetached-Electron Spectra**  
A. Rahman, Iftikhar Ahmad, A. Afaq, M. Haneef, H. J. Zhao
- 083401 Two-Fermion Scattering on Momentum-Representation in a Trap and Their Periodic Phenomena**  
FANG Yi-Zhong, HE Yan-Zhang
- 083701 Photoassociative Production and Detection of Ultracold Polar RbCs Molecules**  
JI Zhong-Hua, ZHANG Hong-Shan, WU Ji-Zhou, YUAN Jin-Peng, ZHAO Yan-Ting, MA Jie, WANG Li-Rong, XIAO Lian-Tuan, JIA Suo-Tang
- FUNDAMENTAL AREAS OF PHENOMENOLOGY(INCLUDING APPLICATIONS)**
- 084101 Proton Acceleration with Double-Layer Targets in the Radiation Pressure Dominant Regime**  
XIA Chang-Quan, DENG Ai-Hua, LIU Li, WANG Wen-Tao, LU Hai-Yang, WANG Cheng, LIU Jian-Sheng
- 084201 Design of a Novel Polarized Beam Splitter Based on a Two-Dimensional Photonic Crystal Resonator Cavity**  
ZHANG Xuan, CHEN Shu-Wen, LIAO Qing-Hua, YU Tian-Bao, LIU Nian-Hua, HUANG Yong-Zhen
- 084202 Single Mode Condition and Power Fraction of Air-Cladding Total Refractive Guided Porous Polymer Terahertz Fibers**  
JING Lei, YAO Jian-Quan
- 084203 Optical Noise Analysis in Dual-Resonator Structural Micro-Optic Gyro**  
YU Huai-Yong, ZHANG Chun-Xi, FENG Li-Shuang, HONG Ling-Fei, WANG Jun-Jie
- 084204 Diode-Pumped Soliton and Non-Soliton Mode-Locked Yb:GYSO Lasers**  
HE Jin-Ping, LIANG Xiao-Yan, LI Jin-Feng, ZHENG Li-He, SU Liang-Bi, XU Jun
- 084205 Optical Properties of BDK-Doped Highly Photosensitive Sol-Gel Hybrid Film**  
XU Ming, SHEN Wei-Dong, ZHANG Yue-Guang, ZHEN Hong-Yu, LIU Xu
- 084206 Large-Mode-Area Double-Cladding Photonic Crystal Fiber Laser in the Watt Range at 980 nm**  
LI Ping-Xue, ZHANG Xue-Xia, LIU Zhi, CHI Jun-Jie
- 084207 A High Power Single Frequency Diode Side-Pumped Nd:YAG Ring Laser**  
XIE Shi-Yong, BO Yong, XU Jia-Lin, WANG Zhi-Chao, PENG Qin-Jun, CUI Da-Fu, XU Zu-Yan
- 084208 Third-Order Optical Nonlinearities of Squarylium Dyes with Benzothiazole Donor Groups Measured Using the Picosecond Z-Scan Technique**  
LI Zhong-Yu, XU Song, CHEN Zi-Hui, ZHANG Fu-Shi, KASATANI Kazuo
- 084209 Reduction of the Far-Field Divergence Angle of an 850 nm Multi-Leaf Holey Vertical Cavity Surface Emitting Laser**  
ZHOU Kang, XU Chen, XIE Yi-Yang, ZHAO Zhen-Bo, LIU Fa, SHEN Guang-Di

- 084210 Light Scattering of Rough Orthogonal Anisotropic Surfaces with Secondary Most Probable Slope Distributions**  
LI Hai-Xia, CHENG Chuan-Fu
- 084211 Experimental Observation of Near-Field Deterioration Induced by Stimulated Rotational Raman Scattering in Long Air Paths**  
WANG Jing, ZHANG Xiao-Min, HAN Wei, LI Fu-Quan, ZHOU Li-Dan, FENG Bin, XIANG Yong
- 084212 Compact 2×2 Multi-Mode Interference Couplers with Uneven Splitting-Ratios Based on Silicon Nanowires**  
ZHOU Jing-Tao, SHEN Hua-Jun, YANG Cheng-Yue, LIU Huan-Ming, TANG Yi-Dan, LIU Xin-Yu
- 084213 Measurement of Temperature Change in Nonlinear Optical Materials by Using the Z-Scan Technique**  
DONG Shu-Guang, YANG Jun-Yi, SHUI Min, YI Chuan-Xiang, LI Zhong-Guo, SONG Ying-Lin
- 084214 A Digital Phase Lock Loop for an External Cavity Diode Laser**  
WANG Xiao-Long, TAO Tian-Jiong, CHENG Bing, WU Bin, XU Yun-Fei, WANG Zhao-Ying, LIN Qiang
- 084301 Nondestructive Characterization of Quantitative Bonding Strength at a Bonded Solid-Solid Interface**  
CHEN Jian-Jun, ZHANG De, MAO Yi-Wei, CHENG Jian-Chun
- 084302 Simultaneous Measurements of Harmonic Waves at Fatigue-Cracked Interfaces**  
Hyunjo Jeong, Dan Barnard
- 084701 MHD Flow of an Oldroyd-B Fluid through a Porous Space Induced by Sawtooth Pulses**  
Masood Khan, Zeeshan
- 084702 Dual Solutions in Unsteady Stagnation-Point Flow over a Shrinking Sheet**  
Krishnendu Bhattacharyya
- 084703 Experimental Investigation of Flow Drag and Turbulence Intensity of a Channel Flow with Rough Walls**  
ZHANG Hui-Qiang, LU Hao, WANG Bing, WANG Xi-Lin
- 084704 Instability Criterion of One-Dimensional Detonation Wave with Three-Step Chain Branching Reaction Model**  
TENG Hong-Hui, JIANG Zong-Lin
- 084705 MHD Boundary Layer Flow of Dilatant Fluid in a Divergent Channel with Suction or Blowing**  
Krishnendu Bhattacharyya, G. C. Layek
- 084706 A Low Voltage Driven Digital-Droplet-Transporting-Chip by Electrostatic Force**  
GAO An-Ran, LIU Xiang, GAO Xiu-Li, LI Tie, GAO Hua-Min, ZHOU Ping, WANG Yue-Lin
- 084707 Peristaltic Motion of Power-Law Fluid with Heat and Mass Transfer**  
T. Hayat, S. Hina, Awatif A. Hendi
- 084708 Direct Numerical Simulation of Particle Migration in a Simple Shear Flow**  
LV Hong, TANG Sheng-Li, ZHOU Wen-Ping
- PHYSICS OF GASES, PLASMAS, AND ELECTRIC DISCHARGES**
- 085201 Preliminary Investigation of a Dielectric Barrier Discharge Lamp in Open Air at Atmospheric Pressure**  
LIU Feng, WANG Wei-Wei, CHANG Xi-Jiang, LIANG Rong-Qing
- 085202 Shock-Timing Experiment Using a Two-Step Radiation Pulse with a Polystyrene Target**  
WANG Feng, PENG Xiao-Shi, JIAO Chun-Ye, LIU Shen-Ye, JIANG Xiao-Hua, DING Yong-Kun
- 085203 Magnetic Fluid Flows in Porous Media**  
LI Ming-Jun, CHEN Liang
- CONDENSED MATTER: STRUCTURE, MECHANICAL AND THERMAL PROPERTIES**
- 086101 Mechanical Property Evaluation of GaAs Crystal for Solar Cells**  
JIN Min, FANG Yong-Zheng, SHEN Hui, JIANG Guo-Jian, WANG Zhan-Yong, XU Jia-Yue



- 086102 Effect of Iodine Additive on Thermostability of Bulk Amorphous Sulfur Prepared by Rapid Compression**  
LIN Sheng-Xiong, LIU Xiu-Ru, SHAO Chun-Guang, SHEN Ru, HONG Shi-Ming
- 086103 Hole Mobility of Molecular  $\beta$ -Copper Phthalocyanine Crystal**  
S. Pengmanayol, T. Osotchan, M. Suewattana, N. Ingadapa, J. Girdpun
- 086104 A Novel Large Moment Antiferromagnetic Order in  $K_{0.8}Fe_{1.6}Se_2$  Superconductor**  
BAO Wei, HUANG Qing-Zhen, CHEN Gen-Fu, M. A. Green, WANG Du-Ming, HE Jun-Bao, QIU Yi-Ming
- 086201 Hydrogenic-Donor Impurity States in  $GaAs/Al_xGa_{1-x}As$  Quantum Dots in the Presence of an Electric Field**  
PAN Jiang-Hong, LIU Li-Zhe, LIU Min
- 086401 FMAA-MS Investigation into  $Ni_{68}Fe_{32}$  Nanoalloy with Sample Length Less than 30 nm**  
LI Ping-Yun, CAO Zhen-Hua, JIANG Zhong-Hao, MENG Xiang-Kang
- 086601 Stability of  $TiO_2$  and  $Al_2O_3$  Nanofluids**  
WANG Xian-Ju, LI Hai, LI Xin-Fang, WANG Zhou-Fei, LIN Fang
- 086602 Elimination of the Coherent Artifact in a Pump-Probe Experiment by Directly Detecting the Background-Free Diffraction Signal**  
LIU Hui, ZHANG Hang, SI Jin-Hai, YAN Li-He, CHEN Feng, HOU Xun
- 086801 Spectral Resolution Improvement of Mo/Si Multilayers**  
WU Wen-Juan, WANG Zhan-Shan, ZHU Jing-Tao, ZHANG Zhong, WANG Feng-Li, CHEN Ling-Yan, ZHOU Hong-Jun, HUO Tong-Lin
- 086802 Structural and Electronic Properties of Sulfur-Passivated  $InAs(001) (2 \times 6)$  Surface**  
LI Deng-Feng, GUO Zhi-Cheng, LI Bo-Lin, DONG Hui-Ning, XIAO Hai-Yan
- 086803 Electrical, Structural and Interfacial Characterization of  $HfO_2$  Films on Si Substrates**  
TAN Ting-Ting, LIU Zheng-Tang, LI Yan-Yan
- CONDENSED MATTER: ELECTRONIC STRUCTURE, ELECTRICAL, MAGNETIC, AND OPTICAL PROPERTIES**
- 087101 Dynamics of Exciton Diffusion in PVK:Phosphorescent Materials/Al Hetero-Structures**  
YANG Shao-Peng, HUANG Da, GE Da-Yong, LIU Bo-Ya, WANG Li-Shun, FU Guang-Sheng
- 087102 Growth and Properties of Blue and Amber Complex Light Emitting  $InGaN/GaN$  Multi-Quantum Wells**  
XIE Zi-Li, ZHANG Rong, LIU Bin, XIU Xiang-Qian, SU Hui, LI Yi, HUA Xue-Mei, ZHAO Hong, CHEN Peng, HAN Ping, SHI Yi, ZHENG You-Dou
- 087103 Electronic Properties of Boron Nanotubes under Uniaxial Strain: a DFT study**  
PAN Li-Jun, JIA Yu, SUN Qiang, HU Xing
- 087201 Current Transport in Copper Schottky Contacts to  $a$ -Plane/ $c$ -Plane n-Type  $MoSe_2$**   
C. K. Sumesh, K. D. Patel, V. M. Pathak, R. Srivastav
- 087301 Leakage Current and Photovoltaic Properties in a  $Bi_2Fe_4O_9/Si$  Heterostructure**  
JIN Ke-Xin, LUO Bing-Cheng, ZHAO Sheng-Gui, WANG Jian-Yuan, CHEN Chang-Le
- 087302 Oscillations of Low-Field Magnetoresistivity of Two-Dimensional Electron Gases in  $Al_{0.22}Ga_{0.78}N/GaN$  Heterostructures in a Weak Localization Region**  
HAN Kui, TANG Ning, DUAN Jun-Xi, LU Fang-Chao, LIU Yu-Chi, SHEN Bo, ZHOU Wen-Zheng, LIN Tie, SUN Lei, YU Guo-Lin, CHU Jun-Hao
- 087303 Transformation from AA to AB-Stacked Bilayer Graphene on  $\alpha$ - $SiO_2$  under an Electric Field**  
LIU Yan, AO Zhi-Min, WANG Tao, WANG Wen-Bo, SHENG Kuang, YU Bin
- 087304 Rectifying Characteristics and Transport Behavior in a Schottky Junction of  $CaCu_3Ti_4O_{12}$  and Pt**  
CHEN Cong, NING Ting-Yin, WANG Can, ZHOU Yue-Liang, ZHANG Dong-Xiang, WANG Pei, MING Hai, YANG Guo-Zhen

- 087305 Influence of Fluorine on the Conductivity and Oxidation of Silicon Nanomembranes after Hydrofluoric Acid Treatment**  
ZHAO Xiang-Fu, HAN Ping, ZHANG Rong, ZHENG You-Dou
- 087306 Dipolar and Quadrupolar Modes of SiO<sub>2</sub>/Au Nanoshell Enhanced Light Trapping in Thin Film Solar Cells**  
BAI Yi-Ming, WANG Jun, CHEN Nuo-Fu, YAO Jian-Xi, ZHANG Xing-Wang, YIN Zhi-Gang, ZHANG Han, HUANG Tian-Mao
- 087401 Influence of Magnetic Scattering and Interface Transparency on Superconductivity Based on a Ferromagnet/Superconductor Heterostructure**  
PENG Lin, LIU Yong-Sheng, CAI Chuan-Bing, ZHANG Jin-Cang
- 087402 Structural, Electronic and Optical Properties of BiAl<sub>x</sub>Ga<sub>1-x</sub>O<sub>3</sub> (x= 0, 0.25, 0.5 and 0.75)**  
GONG Sai, WANG Yue-Hua, ZHAO Xin-Yin, ZHANG Min, ZHAO Na, DUAN Yi-Feng
- 087403 Fabrication of High-Quality Niobium Superconducting Tunnel Junctions**  
XU Qin-Yin, CAO Chun-Hai, LI Meng-Yue, JIANG Yi, ZHA Shi-Tong, KANG Lin, XU Wei-Wei, CHEN Jian, WU Pei-Heng
- 087501 Magnetic Performance of a Nanocomposite Permanent Material**  
LIU Min, HAN Guang-Bing, GAO Ru-Wei
- 087701 Piezoresponse Force Microscopy Imaging of Ferroelectric Domains in Bi(Zn<sub>1/2</sub>Ti<sub>1/2</sub>)O<sub>3</sub>-Pb(Mg<sub>1/3</sub>Nb<sub>2/3</sub>)O<sub>3</sub>-PbTiO<sub>3</sub> Piezoelectric Ceramics**  
LIU Li-Ming, ZENG Hua-Rong, CAO Zhen-Zhu, LENG Xue, ZHAO Kun-Yu, LI Guo-Rong, YIN Qing-Rui
- 087801 Femtosecond Pulse Propagation in a Symmetric Gap Surface Plasmon Polariton Waveguide**  
LU Zhi-Xin, YU Li, LIU Bing-Can, ZHANG Kai, SONG Gang
- 087802 Fast Modification of Microdischarge Emission Bands by Fracture of Sugar**  
Sergej Aman, Juergen Tomas, A. Streletskii
- 087803 Temperature-Induced Phase Transition of In<sub>2</sub>O<sub>3</sub> from a Rhombohedral Structure to a Body-Centered Cubic Structure**  
YANG Lin-Hong, DONG Hong-Xing, SUN Zheng, SUN Liao-Xin, SHEN Xue-Chu, CHEN Zhang-Hai
- 087804 Optical Temperature Sensor Using Infrared-to-Visible-Frequency Upconversion in Er<sup>3+</sup>/Yb<sup>3+</sup>-Codoped Bi<sub>3</sub>TiNbO<sub>9</sub> Ceramics**  
CHEN Heng-Zhi, YANG Bin, SUN Yan, ZHANG Ming-Fu, WANG Zhu, ZHANG Rui, ZHANG Zhi-Guo, CAO Wen-Wu
- 087805 Raman and Mid-IR Spectral Analysis of the Atacamite-Structure Hydroxyl/Deuteroyl Nickel Chlorides Ni<sub>2</sub>(OH/D)<sub>3</sub>Cl**  
LIU Xiao-Dong, Hagihala Masato, ZHENG Xu-Guang, MENG Dong-Dong, GUO Qi-Xin
- CROSS-DISCIPLINARY PHYSICS AND RELATED AREAS OF SCIENCE AND TECHNOLOGY**
- 088101 Floating Zone Growth and Thermionic Emission Property of Single Crystal CeB<sub>6</sub>**  
BAO Li-Hong, ZHANG Jiu-Xing, ZHOU Shen-Lin, ZHANG Ning, XU Hong
- 088301 Modeling of PZT Ferroelectric Ceramic Depolarization Driven by Shock Stress**  
LAN Chao-Hui, PENG Yu-Fei, LONG Ji-Dong, WANG Qiang, WANG Wen-Dou
- 088501 Double-Teeth-Shaped Plasmonic Waveguide Electro-Optical Switches**  
ZHU Jia-Hu, HUANG Xu-Guang, MEI Xian
- 088502 Spin Filtering in a Nanowire Superlattice by Dresselhaus Spin-Orbit Coupling**  
Samad Javidan
- 088701 Electronic Properties of the N<sub>2</sub>C<sub>4</sub> Cluster of DNA**  
WANG Yong-Juan, CHENG Jie, YUE Xian-Fang
- 088702 Estimating RNA Loop Entropies Using a New Nucleobase Model and Sequential Monte Carlo Method**  
LIN Hui, ZHANG Jian

**088703 Viscoelastic Characteristics of Fins, Muscle and Skin in Crucian Carp (*Carassius Auratus*) Described by the Fractional Zener Model**  
CHEN Ming, JIA Lai-Bing, YIN Xie-Zhen

**GEOPHYSICS, ASTRONOMY, AND ASTROPHYSICS**

**089201 Non-Markovian and Non-Perturbative Entanglement Dynamics of Biomolecular Excitons**  
LIU Zhi-Qiang, LIANG Xian-Ting

**089601 Magnetic Reconnection Under Solar Coronal Conditions with the 2.5D AMR Resistive MHD Model**  
ZHANG Shao-Hua, FENG Xue-Shang, WANG Yi, YANG Li-Ping

**089701 PSR J1614-2230 May Include Hyperons**  
YU Zi, DING Wen-Bo, BAO Tmurbagan, LIU Ning-Ning

**089702 Fermi  $\gamma$ -Ray Pulsars: Spectral and Generation Order Parameters**  
CAI Yan, A. Taani, WANG Wei, ZHAO Yong-Heng, ZHANG Cheng-Min

**089801 Inflation and Singularity of a Bianchi Type-VII<sub>0</sub> Universe with a Dirac Field in the Einstein–Cartan Theory**  
HUANG Zeng-Guang, FANG Wei, LU Hui-Qing

**089802 Locally Rotationally Symmetric Bianchi Type-II Magnetized String Cosmological Model with Bulk Viscous Fluid in General Relativity**  
Atul Tyagi, Keerti Sharma

**089803 Bianchi Type-I Massive String Magnetized Barotropic Perfect Fluid Cosmological Model in the Bimetric Theory of Gravitation**  
N. P. Gaikwad, M. S. Borkar, S. S. Charjan

**JUST FOR AUTHORS**  
— CHINESE PHYSICS LETTERS